Bioresource Technology 253 (2018) 297–303

Contents lists available at ScienceDirect

Bioresource Technology

journal homepage: www.elsevier.com/locate/biortech

Bioenergy potential of *Wolffia arrhiza* appraised through pyrolysis, kinetics, thermodynamics parameters and TG-FTIR-MS study of the evolved gases

Muhammad Sajjad Ahmad[b], Muhammad Aamer Mehmood[a,b,*], Chen-Guang Liu[c,*], Abdul Tawab[d], Feng-Wu Bai[c], Chularat Sakdaronnarong[e], Jianren Xu[c], Sawsan Abdulaziz Rahimuddin[f], Munazza Gull[f]

[a] College of Bioengineering, Sichuan University of Science and Engineering, Zigong 643000, China
[b] Bioenergy Research Center, Department of Bioinformatics and Biotechnology, Government College University Faisalabad, Faisalabad 38000, Pakistan
[c] State Key Laboratory of Microbial Metabolism, School of Life Sciences and Biotechnology, Shanghai Jiao Tong University, Shanghai 200240, China
[d] National Institute for Biotechnology and Genetic Engineering, Faisalabad 38000, Pakistan
[e] Department of Chemical Engineering, Mahidol University, Phutthamonthon, Nakhon Pathom 73170 Thailand
[f] Biochemistry Department, Faculty of Science, King Abdulaziz University, Jeddah 21551, Saudi Arabia

GRAPHICAL ABSTRACT

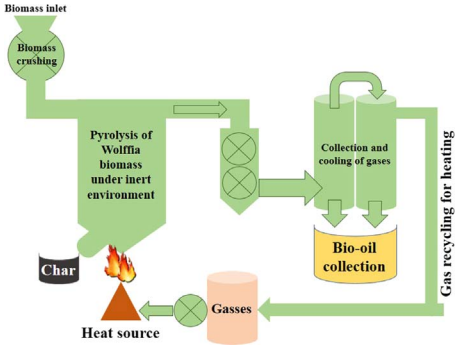

ARTICLE INFO

Keywords:
Wolffia biomass
Pyrolysis
TG-FTIR-MS
Bioenergy
Waste-to-fuel

ABSTRACT

This study evaluated the bioenergy potential of *Wolffia arrhiza* via pyrolysis. The biomass was collected from the pond receiving city wastewater. Oven dried powdered biomass was exposed to thermal degradation at three heating rates (10, 30 and 50° C min^{-1}) using Thermogravimetry–Differential Scanning Calorimetry analyzer in an inert environment. Data obtained were subjected to the isoconversional models of Kissenger-Akahira-Sunose (KSA) and Flynn–Wall–Ozawa (FWO) to elucidate the reaction chemistry. Kinetic parameters including, E_a (136–172 kJmol^{-1}) and Gibb's free energy (171 kJmol^{-1}) showed the remarkable bioenergy potential of the biomass. The average enthalpies indicated that the product formation is favored during pyrolysis. Advanced coupled TG-FTIR-MS analyses showed the evolved gases to contain the compounds containing C=O functional groups (aldehydes, ketones), aromatic and aliphatic hydrocarbons as major pyrolytic products. This low-cost abundant biomass may be used to produce energy and chemicals in a cost-efficient and environmentally friendly way.

* Corresponding authors at: College of Bioengineering, Sichuan University of Science and Engineering, Zigong 643000, China (M.A. Mehmood).
E-mail addresses: draamer@gcuf.edu.pk (M.A. Mehmood), cg.liu@sjtu.edu.cn (C.-G. Liu).

https://doi.org/10.1016/j.biortech.2018.01.033
Received 14 December 2017; Received in revised form 31 December 2017; Accepted 5 January 2018
Available online 13 January 2018

1. Introduction

The finite reserves of fossil fuels and their associated environmental issues have triggered the researchers to find alternative sources of energy to meet increasing global requirements of energy demands of transport and industry. It is estimated that fossil reserves will not be able to fulfill the oil and gas requirements after next 48 to 64 years (Fernandez-Lopez et al., 2016). The Sun is the ultimate source of energy providing 120,000 TW of energy to Earth, which is more than enough when compared to the global energy requirement i.e. 13 TW. Solar energy can be harnessed in two ways, either by storing into photovoltaic cells or photosynthetic fixation into plant biomass which can be later converted into fuels (Liao et al., 2016). In principle, both these approaches are sustainable and cleaner but the storage of electricity produced via solar panels is a big challenge because one kg of biomass can store 27–42 MJ of energy, when compared to lithium-ion batteries which can store only 1–2 MJ kg^{-1} of energy (Liao et al., 2016). Although biomass-based fuel production through biological fermentation has several challenges including difficult hydrolysis yet, owing to its abundance and renewable nature, it is the only foreseeable source of energy, chemicals, and liquid fuels in future (Mehmood et al., 2017a).

Among plant biomass, water born plants are a potential feedstock for biofuel production, because they do not compete with food crops, have higher photosynthetic efficiency and are capable to produce higher oil content when compared to terrestrial crops. Moreover, they are proven to be helpful in the cleaning of wastewater and prevent eutrophication in lakes, water streams and rivers (Duan et al., 2013; Gill et al., 2016). Besides other aquatic plants, duckweed is a tiny, rapidly growing plant which is often found floating on the pond surface. It can extract undesirable minerals like nitrogen, phosphorus, aluminum, potassium and other heavy metals from polluted water. Furthermore, duckweed has higher growth rates when compared to other plants, able to double its biomass within two days. Hence, it can be utilized as a potential feedstock for bioenergy production. Interestingly, duckweeds contain valuable nutrients and its biomass can be used for soil reclamation. Moreover, it has higher production rates and greater photosynthetic activity (Duan et al., 2013). Sun-dried aquatic biomass may also be subjected to thermal conversion to suitable compounds including bio-oils and chemicals.

Pyrolysis is a thermal decomposition process which is usually performed in an inert atmosphere to convert the biomass either into high-value industrial products or to obtain energy. This process depends upon several factors namely temperature, rate of heating, provided pressure, residence time, moisture content of the biomass, particle size of the sample, and its composition (Slopiecka et al., 2012). Though any biomass can be subjected to pyrolysis, however, it is necessary to comprehend the pyrolytic behavior to harness the full potential through pyrolysis. Previously, pyrolytic properties of aquatic biomass namely *Potamogeton crispus* and *Sargassum thunbergii* (Li et al., 2012) have been studied. These biomasses were shown to have different pyrolysis behavior which may be attributed to the difference in their biochemical compositions. Similarly, *Wolffia arrhiza* is a circular floating weed, often found in wastewater. Many of *Wolffia* species are helpful in water purification, able to remove heavy metals from effluent (Suppadit, 2011), producing nutrients and protein-rich biomass which can be used to produce various industrial products. Moreover, *Wolffia* species accumulates the higher amount of starch which makes this weed suitable to produce a variety of biofuels and it can be easily recovered from its medium due to small plant size, thus require less input energy as compared to other aquatic plants which are heavier than *Wolffia*. The present work was focused on understanding the pyrolysis behavior of *W. arrhiza* biomass. The pyrolysis, kinetic, thermodynamic parameters and TG-FTIR-MS study of the evolved gases of pyrolyzed *W. arrhiza* have demonstrated that it has remarkable bioenergy potential.

2. Materials and methods

2.1. Collection of W. arrhiza biomass and proximate analyses

Biomass of *W. arrhiza* (will be referred as Wolffia from now on) was collected from wastewater pond, accumulating municipal waste, mixed with industrial wastes, mainly coming from textile industry. The biomass was washed with tap water to make samples clean. Biomass samples were dried under direct heat of the sun for 3 days. Furthermore, samples were placed in an oven at 110 °C to release further moisture contents and then particle size of 125 μm was obtained through pulverization in plant disintegrator by passing through the mesh. The physicochemical analysis was done to determine the percentage of moisture, ash and volatile matter through standard protocols of ASTM E1755-01 (2007), ASTM E871-82 (2006) and ASTM E872-82 (2006) respectively. However, the percentage of fixed carbon (FC) was obtained by the following formula FC (%) = 100 − (moisture + ash + volatiles). Moreover, samples were pre-weighed to put in an oven for 50 h at 105 °C to estimate the total solid and moisture contents in the sample. Percentage of fixed carbon contents and volatile matter were calculated by placing samples in pre-weighed crucibles in an oven, at 600 °C for 3–4 h, to calculate the difference between before and after heating. All experiments were conducted in triplicate and used average values to ensure precision.

2.2. Calculation of high heating value and determining elemental composition

The elemental composition of C (carbon), H (hydrogen), N (nitrogen), S (Sulphur) and O (oxygen) were obtained by using Ar (argon) as a carrier gas in the elemental analyzer (Vario EL Cube, Germany). All elemental composition was estimated on total dry mass basis. Furthermore, HHV (high heating values) plays an important role to estimate the amount of heat (energy) released from the sample in burning process. However, as an alternative of experimental methods, a few correlation methods have been established for calculating HHV of the sample by using pre-calculated proximate values of the sample. Here, the most reliable correlation model established to date was employed to estimate the HHV of biomass (Nhuchhen and Salam, 2012) of the Wolffia biomass.

2.3. TGA-DSC experiment

Generally, pyrolysis of biomass can be pictured as; $Biomass \rightarrow Liquids + Gases + Char$, however, different pyrolysis reaction conditions are used for different biomasses because of variations in the chemical composition of compounds present in a specific biomass. In the present study, the reaction chemistry of biomass was elucidated using kinetic analyses using the data obtained from coupled Thermogravimetric-Differential Scanning Calorimetry (TG-DSC) analyses. The sample was placed in aluminum crucible (almost 10 mg), three heating rates (10, 30 and 50 °C min^{-1}) were established to study the reaction inside the TG-DSC instrument by observing the mass loss. All experiments were carried out under an inert environment by maintaining a constant flow rate of Nitrogen (100 mL min^{-1}), in the reaction chamber of the equipment (STA-409, NETZSCH-Gerätebau GmbH, Germany).

2.4. Kinetics and thermodynamic parameters calculation

To analyze the TGA-DSC data for establishing the kinetic parameters and to develop mathematical models several methods have been used. In the present study, isoconversional models of KAS (Kissenger-Akahira-Sunose) and FWO (Flynn-Wall-Ozawa) were employed for data analyses (Akahira and Sunose, 1969; Flynn and Wall, 1966; Ozawa, 1965) from the pyrolysis of Wolffia.

Conversion rate in pyrolysis reaction was calculated as;

$$\alpha = (m_o - m_t)/(m_o - m_\infty) \quad (1)$$

where m_o refers to initial mass, m_t is mass at any point of time under observation, and m_∞ refers to the final residual mass.

The decomposition rate of the biomass could be written as;

$$\frac{d\alpha}{dt} = kf(\alpha) \quad (2)$$

where $f(\alpha)$ is the reaction model, and k is the constant. Using Arrhenius temperature dependence of k, Eq. (2) could be written as

$$\frac{d\alpha}{dt} = A\ exp\left(-\frac{E}{RT}\right)f(\alpha) \quad (3)$$

where E = activation energy (kJmol^{-1}), A = pre-exponential factor (s^{-1}), R = universal gas constant and T = absolute temperature (K).

By introducing the heating rate, β, and the conversion function, $f(\alpha) = (1-\alpha)$ Eq. (3) was written as;

$$\frac{d\alpha}{dT} = \frac{A}{\beta}exp\left(-\frac{E}{RT}\right)(1-\alpha) \quad (4)$$

Now, integrated the $\alpha = 0$, at $T = T_0$ as initial conditions in Eq. (4) and after mathematical manipulations, gives

$$G(\alpha) = \int_0^\alpha d\alpha/(1-\alpha) = ART^2/\beta E[1-2RT/E]exp\left(-\frac{E}{RT}\right) \quad (5)$$

After rearranging Eq. (5), $2RT/E$ is approximately equal to unity that can be ignored (Coats and Redfern, 1964), so Eq. (5) becomes

$$G(\alpha) = (ART^2/\beta E)exp(-E/RT) \quad (6)$$

Following two Kinetic methods were used;

2.4.1. KAS method

Kissenger-Akahira-Sunose model was applied to Eq. (6), after rearrangement and taking logarithm of both sides of equation, mathematical expression became;

$$\ln\left(\frac{\beta}{T^2}\right) = ln(AR/EG(\alpha)) - E/RT \quad (7)$$

The left side of the Eq. (7) was put on the y-axis and right-side (1/T) put on the x-axis to plot the graph.

2.4.2. FWO method

FWO method introduced Doyle's approximation (Doyle, 1961). By substituting Doyle's approximation equation and some mathematical approximation Eq. (5) became;

$$\ln(\beta) = ln\left(\frac{AE}{RG(\alpha)}\right) - \frac{E}{RT} \quad (8)$$

The left side of Eq. (8) was plotted against the inverse of pyrolysis temperature to calculate kinetic parameters for any selected α value. Value of conversion rate (α) was used to calculate the value of $A(s^{-1})$ at conversion rate (α). In the plot of $\ln(\beta)$ and $\ln\left(\frac{\beta}{T^2}\right)$ on Y-axis and 1/T on X-axis gave straight lines, that were used to find out the E_a for the progressing values of conversion. Moreover, the thermodynamic parameters namely activation energy (E), enthalpies (ΔH), Gibb's free energy (ΔG), and entropies (ΔS) were calculated using following standard equations.

$$A = [\beta . Eexp(E/RT_m)]/(RT_m^2)$$

$$\Delta H = E - RT$$

$$\Delta G = E_\alpha + RT_m \ln(K_B T_m/hA)$$

$$\Delta S = \Delta H - \Delta G/T_m$$

where:

K_B = Boltzmann Constant ($1.381 \times 10^{-23} J/K$)
h = Plank's Constant($6.626 \times 10^{-34} Js$)
T_m = Temperature in, K

2.5. Coupled TG-FTIR-MS analysis

2.5.1. FTIR analysis

Chemical groups and real-time compounds were detected through coupled TG-FTIR-GCMS analyzer using 5 mg biomass. This biomass sample was treated in thermogravimetric analyzer connected with the FTIR-GCMS (PerkinElmer, Model: TGIRGCMS*/TGA8000*). The aim was to identify the mass losses, functional groups and other kinetic parameters of sample components of thermally treated biomass (Luo et al., 2017). The range of spectral resolution was selected from 400 to 4000 Wavenumber (cm^{-1}), while the data acquisition frequency was set at 8 s. The temperature of the thermogravimetric analyzer was ramped from 50 °C to 800 °C before FTIR-MS analysis.

2.5.2. GC–MS analysis

The volatile components passed through FTIR, were instantly analyzed using coupled GC–MS. The analysis was conducted at 70 eV using positive electron impact (EI) mode. The injector temperature was 150 °C. The thermal programming of the oven was set at an initial 50 °C temperature for 3 min, followed by a smooth ramping at 10 °Cmin^{-1} to 280 °C. The final holding time at 280 °C was 5 min. The temperature of both ion source and transfer line was 50 °C. The separation was conducted using 30 m × 250 μm TR-5MS column. To identify the volatile compounds, the mass spectra, obtained through GC–MS were blasted using NIST library.

3. Results and discussion

3.1. Physiochemical properties

The elemental composition of the Wolffia biomass showed the 35.55% C, 6.36% H, 5.25% N, 1.16% S and 35.87% O based on total dried mass. The higher amounts of Nitrogen and Sulphur indicate the higher amount of protein content and removal of more nutrients from the wastewater. Proximate analyses of Wolffia have shown that its biomass contains moisture content up to 4.76 ± 0.14% which echoes its appropriateness for pyrolysis, while a suitable range of moisture content in biomass is designated as < 10%. The volatile matter of Wolffia was shown to be 72.6% which is higher than water plant *Potamogeton crispus* (60.03%), a macroalgae *Ulva pertusa* (59.3%) and lower than maize straw (78.0%), Para grass (79%) and *Miscanthus gigantus* 78.8% (Ahmad et al., 2017; Jeguirim et al., 2010; Li et al., 2012; Ye et al., 2010). Moreover, the biomass showed 10.4% of ash content. Calculated HHV value of Wolffia was shown to be as 17.77 MJ kg^{-1} which is comparable when compared with renowned bioenergy crops including Giant reed, Miscanthus, *Ulva pertusa*, Para grass, and Maize straw (Jeguirim et al., 2010; Ye et al., 2010; Ahmad et al., 2017).

3.2. Thermal degradation pattern

Pyrolysis experiments were executed at three heating rates, because different heating rates may be useful to obtain different products from the pyrolysis (Ceranic et al., 2016). Thermal behavior of Wolffia has shown in DTG and TG curves (Fig. 1A) which indicate physiochemical changes, taking place during thermal conversion of its biomass into various products (Ceylan and Kazan, 2015; Maia and de Morais, 2016). TG curves have shown the characteristic advent of biomass degradation likewise the DTG curves produced for the pyrolysis of other lignocellulosic biomass such as *Tecktona grandis*, olive mill waste, date palm waste and non-woody lignocellulose (Balogun et al., 2014; Benavente and Fullana, 2015; Bousdira et al., 2017; Demirbas, 2017).

Mass loss pattern of Wolffia could be divided into three stages

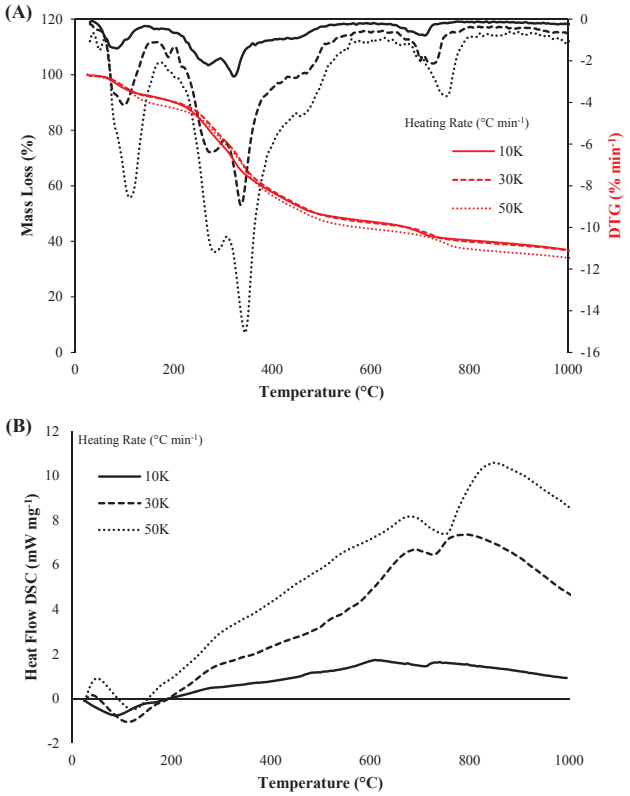

Fig. 1. TG-DTG (A) and DSC (B) curves indicating the percent mass losses in response to three heating rates and heat flow to-and-from the biomass, respectively.

Table 1
Characteristics temperatures associated with the pyrolysis of Wolffia biomass.

Heating rate (°C min^{-1})	Temperature (°C)				
	T1	*T2*	*T3*	*T4*	*T5*
10	155	271	294	321	551
30	159	272	306	336	560
50	170	282	309	344	569

Table 2
Gradual mass losses during thermal degradation stages.

Stages		Heating rate (°C min^{-1})		
		10	30	50
Stage-I, WL (%)		7.77	8.18	10.9
Stage-II, WL (%)	Zone-I	16.88	15.76	15.06
	Zone-II	27.13	28.54	28.92
Stage-III, WL (%)		12.32	11.81	12.11
Final residues at 1000 °C (%)		35.90	35.71	33.01

(Tables 1 and 2) and a long tail. The first stage occurred when temperature increased from ambient to *T1* (155–170 °C) where a 7.70–10% loss in mass was observed. This stage indicates the loss of cellular and surface adsorbed water. Whereas, biomass with retained moisture up to 10% is considered as valuable for combustion (Braga et al., 2014). The second stage may be referred as devolatilization stage, where most of the thermal transformation happened. It ranged from *T1* (170 °C) to *T5* (569 °C). A variety of volatiles would have been released during this stage, resulting in a drastic mass loss, degradation of cellulose and hemicellulose, along with the formation of the major pyrolytic products. This stage could be further subdivided into two degradation zones which could be ascribed to the existence of different stable thermal components in the Wolffia biomass (Li et al., 2012). The third stage is mainly associated with the degradation of lignin component and formation of char. Temperature ranged along with tail from 570 to 800 °C showed approximately 12% mass loss which mainly corresponds to the lignin decomposition. Here lignin mainly contributed towards biochar production as a higher content of lignin in biomass, resulting in high biochar production and higher thermal stability (Bousdira et al., 2017; Braga et al., 2014). Final residues ranged from 33.1 to 35.9% at 1000 °C which indicated the considerably higher amount of char produced, which imitates the fitness of Wolffia for char production.

3.3. Measurement of heat flow to-and-from the Wolffia biomass

The flow of heat to-and-from the Wolffia biomass (mW mg^{-1}) was shown to increase with the increment in the reaction temperature which can be clearly seen as the curves attained through DSC (Fig. 1B). An increasing heat flow at initial stages followed by a decreasing heat flow indicate the range of associated temperatures at different heating rates. First small peaks of endothermic and exothermic reactions were observed at a temperature below than 200 °C. With the increase in temperature exothermic effect increased. Exothermic effect extended up to 700 °C, 750 °C, and 780 °C, for the heating rates of 10, 30 and 50 °C min^{-1} respectively. These observations are in good agreement with the heat flow curves previously constructed for the *S. thunbergii, P. crispus* and Para grass (Ahmad et al., 2017; Li et al., 2012). However, with the further increase in temperature caused a gradual shift in the curves towards the x-axis indicating the that either the reaction was stopped due to depletion of reactants or the reaction followed different mechanism owing to the changing composition of the residual biomass.

3.4. Kinetics and thermodynamic variables

Determining kinetic parameters is critically important to understand and optimize the process of thermal decomposition of biomass into desired products. So, keeping in view their importance kinetic parameters including, pre-exponential factors and activation energy were calculated from the slopes obtained when conversion points were plotted against the inverse of pyrolysis temperature (Fig. 2). The corresponding E_a (activation energies) and preexponential factors (s^{-1}) at each point were calculated. The E_a values (Table 3) showed fluctuations related to conversion points; it revealed the complex nature of samples or reactions occur during the pyrolysis process. Moreover, E_a values were shown to be decreasing with the increasing conversion rates (Fig. 3A). However, the conversion rate (α) displayed a direct relationship with the reaction temperature (Fig. 3B). The average E_a values of Wolffia were revealed to be ranging from 168.35 to 170.37 kJmol^{-1} which were lower than Elephant grass (218–227 kJmol^{-1}), rice husk (221–229 kJmol^{-1}), *Laminaria japonica* (173.2–225.7 kJmol^{-1}), Tobacco waste (118–257 kJmol^{-1}), agricultural residues (220–221 kJmol^{-1}), *Phragmites australis* (291 kJmol^{-1}), *Sargassum pallidum* (203.5 kJmol^{-1}) (Braga et al., 2014; Li et al., 2010; Wu et al., 2015; Wang et al., 2016; Du et al., 2012; Li et al., 2010) and higher than that of *Ulva pertusa* (152–147 kJ mol^{-1}), Camel grass (168–169 kJmol^{-1}), Sewage Sludge and coffee ground mixture (166–168 kJmol^{-1}), Pepper waste (29–147 kJmol^{-1}), Cattle manure (122–124 kJmol^{-1}), Pine (122–169 kJmol^{-1}), and *Dunaliella tertiolecta* (145.7 kJmol^{-1}), (Ye et al., 2010; Mehmood et al., 2017b; Chen et al., 2017a,b; Maia and de Morais, 2016; Wilk et al., 2017; Shuping et al., 2010). These values indicated that feasibility of biomass for co-pyrolysis with several other biomass sources.

Enthalpy of reaction is characterized by the amount of heat exchanged between the reagent and activated complex during the thermal process (Xu and Chen, 2013). When the values of enthalpies (Δ*H*) of Wolffia biomass were compared with values of E_α, a slight difference (~5 kJ mol^{-1}) was found at each conversion point (α) which exhibited that the product formation is being favored due to lower potential energy (Vlaev et al., 2007). The preexponential values (*A*) for Wolffia ranged from 1.14×10^{10}–4.46×10^{14} s^{-1} to 1.04×10^{10}–9.59×10^{13} s^{-1}, estimated

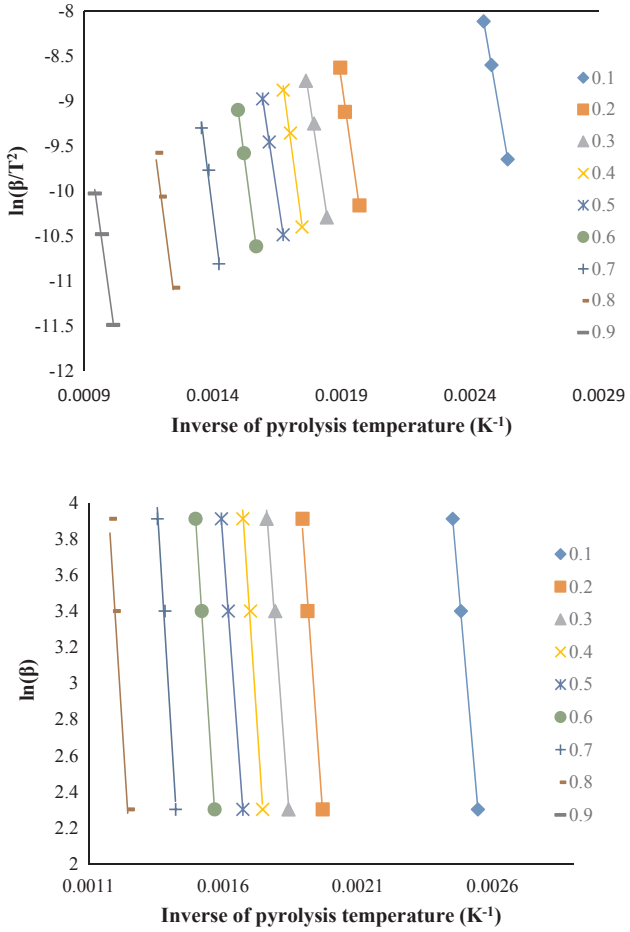

Fig. 2. Linear fit plots to calculate the activation energy of Wolffia: Where, In (β/T2) (KAS Method), and In(β) (FWO method) were plotted against inverse of pyrolysis temperature (K^{-1}).

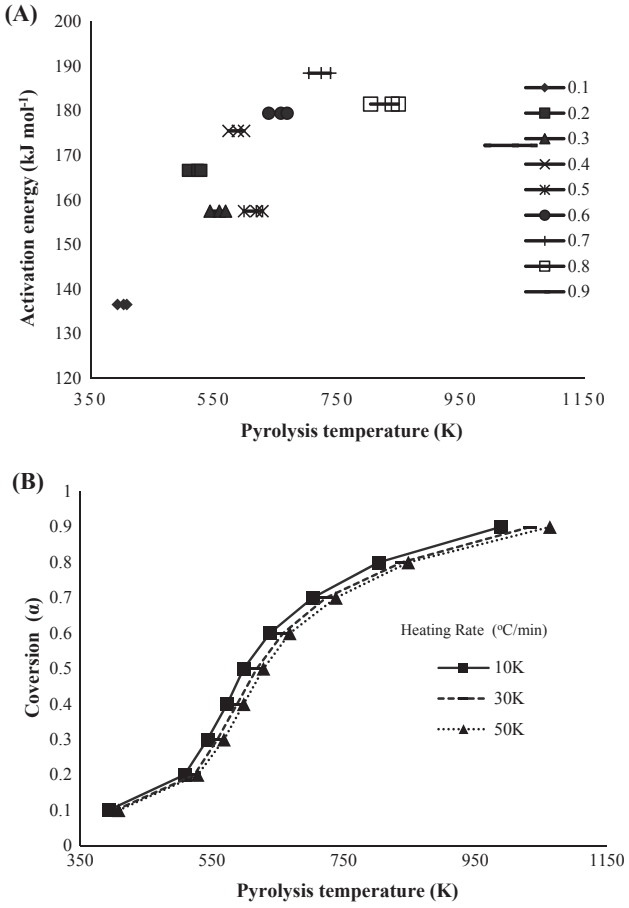

Fig. 3. Relationship of activation energy with pyrolysis temperature (A), and relationship between the conversion (a) and the reaction temperature (B).

Table 3
Kinetics and thermodynamic parameters for the pyrolysis of Wolffia biomass.

α	*Ea* kJmol^{-1}	R^2	*ΔH* kJmol^{-1}	*A* s^{-1}	*ΔG* kJmol^{-1}	*ΔS* Jmol^{-1}
KAS method						
0.1	136.53	0.99	131.47	1.14×10^{10}	172.06	−66.65
0.2	166.62	0.99	161.56	5.29×10^{12}	171.05	−15.59
0.3	157.47	0.99	152.40	8.20×10^{11}	171.34	−31.09
0.4	175.48	0.99	170.41	3.20×10^{13}	170.79	−0.62
0.5	157.48	0.98	152.41	8.21×10^{11}	171.34	−31.08
0.6	179.44	0.99	174.38	7.17×10^{13}	170.68	6.08
0.7	188.45	0.98	183.38	4.46×10^{14}	170.43	21.27
0.8	181.50	0.98	176.44	1.09×10^{14}	170.62	9.56
0.9	172.21	0.99	167.14	1.65×10^{13}	170.89	−6.14
Avg.	**168.35**	–	**163.29**	–	–	–
FWO method						
0.1	136.11	0.99	131.05	1.04×10^{10}	172.08	-67.37
0.2	166.56	0.99	161.50	5.23×10^{12}	171.05	−15.69
0.3	158.46	0.99	153.39	1.00×10^{12}	171.31	−29.42
0.4	176.05	0.99	170.98	3.60×10^{13}	170.77	0.35
0.5	159.36	0.98	154.30	1.21×10^{12}	171.28	−27.88
0.6	180.88	0.99	175.81	9.59×10^{13}	170.64	8.50
0.7	190.50	0.99	185.44	6.76×10^{14}	170.37	24.74
0.8	185.56	0.99	180.49	2.48×10^{14}	170.51	16.40
0.9	179.87	0.99	174.81	7.82×10^{13}	170.67	6.81
Avg.	**170.37**	–	**165.31**	–	–	–

by KAS and FWO methods, respectively (Table 3). While, the (A) $< 10^9\,s^{-1}$ mainly shows the surface reaction whereas (A) $\geq 10^9\,s^{-1}$ shows a simpler complex (Turmanova et al., 2008). Furthermore, A-values of Wolffia were close to A-values calculated for rice straw ($1.70 \times 10^{07}\,s^{-1}$ to $9.35 \times 10^{12}\,s^{-1}$), rice bran ($1.00 \times 10^{07}\,s^{-1}$ and $1.58 \times 10^{10}\,s^{-1}$), Para grass ($1.42 \times 10^{07}$–$2.26 \times 10^{19}\,s^{-1}$) and Camel grass ($2.25 \times 10^{06}$–$5.69 \times 10^{14}\,s^{-1}$) (Ahmad et al., 2017; Biney et al., 2015; Mehmood et al., 2017b).

Changes of entropies (ΔS) for Wolffia had both negative and positive values as well. The minimum negative value of ΔS was $-67.37\,J\,mol^{-1}$ respectively while maximum positive value was $24.74\,J\,mol^{-1}$. Negative entropies specify more arrangement in the activated complex when compared with biomass while positive values show otherwise (Xu and Chen, 2013). The co-occurrence of both in any pyrolysis reaction proposes that this particular thermal conversion would have been relatively complex. The Gibb's free (ΔG) energy exhibits the internal energy of the system (biomass in this case) displayed during the reaction progress. The ΔG values for the pyrolysis of Wolffia were ranged from 170 to $172\,kJ\,mol^{-1}$ which were higher when compared to red pepper waste ($139.4\,kJ\,mol^{-1}$) and rice straw ($164.59\,kJ\,mol^{-1}$) (Maia and de Morais, 2016; Xu and Chen, 2013). Overall reaction chemistry depicted that Wolffia biomass consumes lesser amount of external heat input and improves the stability of the overall process, hence its thermal conversion would be an energy efficient process.

3.5. TG-FTIR-GCMS analysis

The characteristic absorptions for most of the identified compounds were ranging from 700 to $1200\,cm^{-1}$, 1500 to $1900\,cm^{-1}$ followed by 2200 to $2400\,cm^{-1}$ and 3000 to $3800\,cm^{-1}$, based on their specific

Table 4
List of compounds released upon the pyrolysis of Wolffia biomass.

Sr. No	Compound	Formula	Molar mass	CAS No.
1	Toluene	C_7H_8	92	108-88-3
2	L-cystine	$C_6H_{12}N_2O_4S_2$	240	534-22-5
3	Methyl phenyl sulfide, 4-acetamido-S-[(p-toluenesulfonyl)imino]-	$C_{16}H_{18}N_2O_3S_2$	350	28,075-40-3
4	2,3,4-Trimethoxy-6-nitrobenzoic acid	$C_{10}H_{11}NO_7$	257	61,948-84-3
5	Gentamicin A	$C_{18}H_{36}N_4O_{10}$	469	13,291-74-2
6	12-Hydroxy-14-methyl-oxa-cyclotetradec-6-en-2-one	$C_{14}H_{24}O3$	240	77,761-61-6
7	3,4,5-Trimethoxybenzylamine	$C_{10}H_{15}NO_3$	197	18,638-99-8
8	Boranamine, 1-chloro-1-ethyl-N-methyl-N-phenyl-	$C_9H_{13}BClN$	181	55,702-64-2
9	1-Diphenylsilyloxyoctane	$C_{20}H_{28}OSi$	313	99,221-40-6
10	Cephaloridine	$C_{19}H_{17}N_3O_4S_2$	415	50-59-9
11	4-Chlordehydromethyltestosterone	$C_{20}H_{27}ClO_2$	335	2446-23-3
12	Cyclobutene, 2-propenylidene-	C_7H_8	92	52,097-85-5
13	3-Diphenyl(methyl)silyloxypropene	$C_{16}H_{18}OSi$	254	17,933-45-8
14	Neblininediol 21-acetate	$C_{25}H_{32}N_2O_5$	441	54,658-05-8
15	Acetamide, N-methyl-N-[4-(3-hydroxypyrrolidinyl)-2-butynyl]-	$C_{11}H_{18}N$	210	130,403-61-1
16	Glycine, N-(N-glycyl-L-leucyl)-	$C_{10}H_{19}N_3O_4$	245	2576-67-2
17	18-Benzyl-1,4,10,13-tetraoxa-7,16-diazacyclooctadecane-2,6,17-trione	$C_{15}H_{24}O_2$	236	1,005,284-62-7
18	2,2-Dimethyl-4-(2-methyl-1-propenyl)-5-oxo-2,5-dihydro-3-furancarboxylic acid	$C_{11}H_{14}O_4$	210	96,484-50-3
19	Spiculesporic acid	$C_{17}H_{28}O_6$	328	469-77-2
20	Acetamide, N-methyl-N-[4-[2-acetoxymethyl-1-pyrrolidyl]-2-butynyl]-	$C_{14}H_{22}N_2O_3$	266	132,377-28-7
21	1,1-Dichloro-2-methyl-3-(4,4-diformyl-1,3-butadien-1-yl)cyclopropane	$C_{10}H_{10}Cl_2O_2$	233	132,607-16-0
22	2-(2-Carboxyethyl)-6,6-dimethyl-3-oxocyclohex-1-enecarboxylic acid	$C_{12}H_{16}O_5$	240	57,304-91-3
23	(1E,4E)-2,2,5-Trimethyl-5-cycloheptene-1,4-dione dioxime	$C_{10}H_{16}N_2O_2$	196	58,870-13-6
24	2-Trimethylstannyl-5-trichloromethyl-6-chlorobicyclo[2.2.1]heptane	$C_{11}H_{18}Cl_4Sn$	411	74,229-37-1
25	4-(3,3-Dimethyl-but-1-ynyl)-4-hydroxy-2,6,6-trimethylcyclohex-2-enone	$C_{15}H_{22}O_2$	234	930,090-10-1
26	(3aS,6abeta,9bbeta)-3abeta,4,5,6,6a,7,8,9,9a,9b-Decahydro-7beta,9beta-dihydroxy-6alpha,9aalpha-dimethyl-3-methyleneazuleno[4,5-b]furan-2(3H)-	$C_{15}H_{22}O_4$	266	20,555-03-7
27	4-O-[(2S)-3alpha-(Acetylamino)-6-(aminomethyl)-3,4-dihydro-2H-pyran-2alpha-yl]-6-O-[3-deoxy-4-C-methyl-3-(methylamino)-beta-L-arabinopyranosyl]-2-deoxy-D-streptamine	$C_{21}H_{39}N_5O_8$	490	55,649-82-6

kinetic energies associated with their structural and functional groups movements. The strong stretching at 600–800 cm^{-1}, shows halides (C—Cl). The bending at 675 cm^{-1} is for ═C—H of an alkene, also appeared in stretching at 3000–3100 cm^{-1} while 805–835 cm^{-1} is the typical replication of aromatic compounds. The existence of 1031 cm^{-1} shows the deformation of cellulosic moieties while the presence of Aldehydes or Ketones at 1550 to 1600 cm^{-1} and 1600–1628 cm^{-1}, 1700–1750 cm^{-1} indicate the C═O stretching vibrational energies along with carboxylic carbonyl groups, also appearing at 2250 to 2300 cm^{-1}. The stretching at 3000 cm^{-1} identifies the aromatic C—H. Similarly, the free stretching, at 3500–3700 CM^{-1} is noticeable for the O—H functional activity along with amides. The mononuclear hydrocarbons were noticed at 1400–1500 cm^{-1} skeletal vibration, together with out-of-plane C—H bending vibrations at 670 and 910 cm^{-1}.

Through GC–MS around 27 compounds and their thermally decomposed components obtained from biomass were detected (Table 4). The GC–MS results show the presence of many of the components obtained from the Wolffia biomass having high energy toluene and benzene ring containing products e.g 3,4,5-Trimethoxybenzylamine as well as components with functional groups like acetylene e.g Acetamide, N-methyl-N-[4-[2-acetoxymethyl^{-1}-pyrrolidyl]-2-butynyl]- etc. The calorific (Higher Heating) values of toluene, benzene, and acetylene are in the order of 40.6, 41.8 and 49.9 MJ Kg^{-1} comparable to diesel and gasoline with 44.8 and 47.3 MJ Kg^{-1} respectively. This can be theoretically extrapolated to have efficient energy-yielding capacity in terms of usage as fuel. Hence, it has been demonstrated that the *W. arrhiza* biomass can be used to produce bioenergy and chemicals *via* pyrolysis without any direct competition with the food, fodder or arable soil, in a cost and environmentally efficient manner.

4. Conclusions

W. arrhiza is adapted to wastewater, offering a freely accessible biomass for bioenergy with concomitant nutrient-removal. Its pyrolysis comprised of three stages. The stage-1 depicted the evaporation of retained moisture. Whereas, the stage-2 showed drastic mass loss associated with the degradation of carbohydrates indicating that temperature of 271–600 °C may be used for its thermal conversion. While the stage-3 indicated lignin degradation and charring. The TG-FTIR-MS analyses verified the production of energy and industrially valuable chemicals. Its thermodynamic properties indicated a promising bioenergy potential when compared to terrestrial plants making it a potential feedstock in future energy production scenario.

Acknowledgements

Authors are obliged to Higher Education Commision (HEC) Pakistan, International Foundation of Science Sweden and National Natural Science Foundation of China (Grant Numbers: 51561145014, 21536006, 21406030) for their financial support.

References

Ahmad, M.S., Mehmood, M.A., Al Ayed, O.S., Ye, G., Luo, H., Ibrahim, M., Rashid, U., Nehdi, I.A., Qadir, G., 2017. Kinetic analyses and pyrolytic behavior of Para grass (*Urochloa mutica*) for its bioenergy potential. Bioresour. Technol. 224, 708–713.
Akahira, T., Sunose, T. 1969. Transactions of Joint Convention of Four Electrical Institutes, 246.
Balogun, A.O., Lasode, O.A., McDonald, A.G., 2014. Devolatilisation kinetics and pyrolytic analyses of *Tectona grandis* (teak). Bioresour. Technol. 156, 57–62.
Benavente, V., Fullana, A., 2015. Torrefaction of olive mill waste. Biomass Bioenergy 73, 186–194.
Biney, P.O., Gyamerah, M., Shen, J., Menezes, B., 2015. Kinetics of the pyrolysis of arundo, sawdust, corn stover and switch grass biomass by thermogravimetric analysis using a multi-stage model. Bioresour. Technol. 179, 113–122.
Bousdira, K., Bousdira, D., Bekkouche, S.M.E.A., Nouri, L.H., Legrand, J., 2017. Kinetic pyrolysis study and classification of date palm biomass. J. Renew. Sustain. Energy 9, 013102.
Braga, R.M., Melo, D.M., Aquino, F.M., Freitas, J.C., Melo, M.A., Barros, J.M., Fontes, M.S., 2014. Characterization and comparative study of pyrolysis kinetics of the rice husk and the elephant grass. J. Therm. Anal. Calorim. 115, 1915–1920.
Ceranic, M., Kosanic, T., Djuranovic, D., Kaludjerovic, Z., Djuric, S., Gojkovic, P., Bozickovic, R., 2016. Experimental investigation of corn cob pyrolysis. J. Renew. Sustain. Energy 8, 063102.
Ceylan, S., Kazan, D., 2015. Pyrolysis kinetics and thermal characteristics of microalgae *Nannochloropsis oculata* and *Tetraselmis* sp. Bioresour. Technol. 187, 1–5.
Chen, G., He, S., Cheng, Z., Guan, Y., Yan, B., Ma, W., Leung, D.Y.C., 2017a. Comparison of kinetic analysis methods in thermal decomposition of cattle manure by

thermogravimetric analysis. Bioresour. Technol. 243, 69–77.
Chen, J., Liu, J., He, Y., Huang, L., Sun, S., Sun, J., Chang, K., Kuo, J., Huang, S., Ning, X., 2017b. Investigation of co-combustion characteristics of sewage sludge and coffee grounds mixtures using thermogravimetric analysis coupled to artificial neural networks modeling. Bioresour. Technol. 225, 234–245.
Coats, A., Redfern, J., 1964. Kinetic parameters from thermogravimetric data. Nature 201, 68–69.
Demirbas, A., 2017. Higher heating values of lignin types from wood and non-wood lignocellulosic biomasses. Energy Sour. A Recov. Util. Environ. Eff. 39, 592–598.
Doyle, C., 1961. Kinetic analysis of thermogravimetric data. J. Appl. Polym. Sci. 5, 285–292.
Du, J., Yuan, Y., Si, T., Lian, J., Zhao, H., 2012. Customized optimization of metabolic pathways by combinatorial transcriptional engineering. Nucl. Acids Res. 40 e142 e142.
Duan, P., Chang, Z., Xu, Y., Bai, X., Wang, F., Zhang, L., 2013. Hydrothermal processing of duckweed: effect of reaction conditions on product distribution and composition. Bioresour. Technol. 135, 710–719.
Fernandez-Lopez, M., Pedrosa-Castro, G., Valverde, J., Sanchez-Silva, L., 2016. Kinetic analysis of manure pyrolysis and combustion processes. Waste Manage 58, 230–240.
Flynn, J.H., Wall, L.A., 1966. A quick, direct method for the determination of activation energy from thermogravimetric data. J. Poly. Sci. B: Poly. Lett. 4, 323–328.
Gill, S.S., Mehmood, M.A., Ahmad, N., Ibrahim, M., Rashid, U., Ali, S., Nehdi, I.A., 2016. Strain selection, growth productivity and biomass characterization of novel microalgae isolated from fresh and wastewaters of upper Punjab, Pakistan. Front. Life Sci. 9, 190–200.
Jeguirim, M., Dorge, S., Trouve, G., 2010. Thermogravimetric analysis and emission characteristics of two energy crops in air atmosphere: *Arundo donax* and *Miscanthus giganthus*. Bioresour. Technol. 101, 788–793.
Li, D., Chen, L., Chen, S., Zhang, X., Chen, F., Ye, N., 2012. Comparative evaluation of the pyrolytic and kinetic characteristics of a macroalga (*Sargassum thunbergii*) and a freshwater plant (*Potamogeton crispus*). Fuel 96, 185–191.
Li, D., Chen, L., Yi, X., Zhang, X., Ye, N., 2010. Pyrolytic characteristics and kinetics of two brown algae and sodium alginate. Bioresour. Technol. 101, 7131–7136.
Liao, J.C., Mi, L., Pontrelli, S., Luo, S., 2016. Fuelling the future: microbial engineering for the production of sustainable biofuels. Nat. Rev. Microbiol. 14, 288–304.
Luo, L., Liu, J., Zhang, H., Ma, J., Wang, X., Jiang, X., 2017. TG-MS-FTIR study on pyrolysis behavior of superfine pulverized coal. J. Anal. Appl. Pyrol. 128, 64–74.
Maia, A.A.D., de Morais, L.C., 2016. Kinetic parameters of red pepper waste as biomass to solid biofuel. Bioresour. Technol. 204, 157–163.
Mehmood, M.A., Ibrahim, M., Rashid, U., Nawaz, M., Ali, S., Hussain, A., Gull, M., 2017a. Biomass production for bioenergy using marginal lands. Sustain. Prod. Consum. 9, 3–21.
Mehmood, M.A., Ye, G., Luo, H., Liu, C., Malik, S., Afzal, I., Xu, J., Ahmad, M.S., 2017b. Pyrolysis and kinetic analyses of Camel grass (*Cymbopogon schoenanthus*) for bioenergy. Bioresour. Technol. 228, 18–24.
Nhuchhen, D.R., Salam, P.A., 2012. Estimation of higher heating value of biomass from proximate analysis: a new approach. Fuel 99, 55–63.
Ozawa, T., 1965. A new method of analyzing thermogravimetric data. Bull. Chem. Soc. Jpn. 38, 1881–1886.
Shuping, Z., Yulong, W., Mingde, Y., Chun, L., Junmao, T., 2010. Pyrolysis characteristics and kinetics of the marine microalgae *Dunaliella tertiolecta* using thermogravimetric analyzer. Bioresour. Technol. 101, 359–365.
Slopiecka, K., Bartocci, P., Fantozzi, F., 2012. Thermogravimetric analysis and kinetic study of poplar wood pyrolysis. Appl. Energy 97, 491–497.
Suppadit, T., 2011. Nutrient removal of effluent from quail farm through cultivation of *Wolffia arrhiza*. Bioresour. Technol. 102, 7388–7392.
Turmanova, S.C., Genieva, S., Dimitrova, A., Vlaev, L., 2008. Non-isothermal degradation kinetics of filled with rise husk ash polypropene composites. Exp. Poly. Lett. 2, 133–146.
Vlaev, L., Georgieva, V., Genieva, S., 2007. Products and kinetics of non-isothermal decomposition of vanadium (IV) oxide compounds. J. Therm. Anal. Calorim. 88, 805–812.
Wang, X., Hu, M., Hu, W., Chen, Z., Liu, S., Hu, Z., Xiao, B., 2016. Thermogravimetric kinetic study of agricultural residue biomass pyrolysis based on combined kinetics. Bioresour. Technol. 219, 510–520.
Wilk, M., Magdziarz, A., Gajek, M., Zajemska, M., Jayaraman, K., Gokalp, I., 2017. Combustion and kinetic parameters estimation of torrefied pine, acacia and *Miscanthus giganteus* using experimental and modelling techniques. Bioresour. Technol. 243, 304–314.
Wu, W., Mei, Y., Zhang, L., Liu, R., Cai, J., 2015. Kinetics and reaction chemistry of pyrolysis and combustion of tobacco waste. Fuel 156, 71–80.
Xu, Y., Chen, B., 2013. Investigation of thermodynamic parameters in the pyrolysis conversion of biomass and manure to biochars using thermogravimetric analysis. Bioresour. Technol. 146, 485–493.
Ye, N., Li, D., Chen, L., Zhang, X., Xu, D., 2010. Comparative studies of the pyrolytic and kinetic characteristics of maize straw and the seaweed *Ulva pertusa*. PloS One 5, e12641.